Probing Segmental Mobility in the Cyanogenic Glycoside Amygdalin by ^{13}C Solid-State NMR

Göran Widmalm,[†] Kjell Jansson,[‡] Gustav Pellijeff,[§] and Dick Sandström*[,§]

Department of Organic Chemistry, Division of Inorganic Chemistry, and Division of Physical Chemistry, Arrhenius Laboratory, Stockholm University, SE-106 91 Stockholm, Sweden

Received: February 5, 2003; In Final Form: June 4, 2003

Local motions in the cyanogenic glycoside amygdalin have been characterized by variable-temperature ^{13}C solid-state NMR spectroscopy. Carbon-13 chemical shift tensors and $^{1}H-^{13}C$ dipolar couplings were measured by advanced magic-angle spinning NMR techniques over the temperature range 0−90 °C. The main conclusions from our study are that the phenyl ring exhibits thermally activated dynamics about the para axis, whereas the glucopyranosyl residues remain immobile upon heating. It was also found that sample heating is accompanied by loss of water. The experimental results were complemented by quantum chemical calculations of the ^{13}C chemical shift tensors, which were utilized in the analysis of the experimental NMR parameters.

1. Introduction

Amygdalin ((*R*)-1-cyano-1-(phenylmethyl)-*β*-D-glucopyranosyl-(1→6)-*β*-D-glucopyranoside) (shown in Figure 1) is a naturally occurring cyanogenic glycoside found in many food plants.[1] For example, the kernels of apples, almonds, peaches, cherries, and apricots contain this compound. Upon cyanogenesis, amygdalin releases cytotoxic hydrogen cyanide, and accidental acute cyanide poisoning from food is therefore not uncommon.[2] Amygdalin is also the active substance in *laetrile*, a highly controversial anticancer agent.[3]

Despite its biochemical and pharmaceutical significance, little is known about amygdalin's molecular characteristics. The ^{1}H and ^{13}C nuclear magnetic resonance (NMR) spectra of this glycoside have been obtained and assigned in solution,[4] but the details of the molecular structure and dynamics remain to be determined. To the best of our knowledge, the crystal structure of amygdalin is, for example, not known.

In the present work, we report a solid-state NMR study of amygdalin. The focus of the investigation is to determine the segmental mobility as a function of temperature. Deuterium (^{2}H) NMR spectroscopy has traditionally been the standard technique to study local dynamics in solid systems.[5−8] The major advantage of ^{2}H NMR is that it produces simple and intense spectra but has the disadvantage that site-specific isotopic labeling is required. Another popular approach is to measure ^{1}H and ^{13}C nuclear spin relaxation rates.[9−11] Unfortunately, the analysis of relaxation times in terms of the rate and geometry of molecular motions in solids is often quite complex. To avoid the above-mentioned problems, we have used various high-resolution solid-state NMR methods to obtain ^{13}C chemical shift (CS) tensor components and $^{1}H-^{13}C$ through-space dipolar couplings. Magic-angle spinning (MAS) provides in these experiments high sensitivity and chemical-site resolution, and it is therefore possible to apply the techniques to powdered samples with ^{13}C in natural abundance. The experimental results were complemented by quantum chemical calculations of the ^{13}C CS tensors. These calculations provide data that are useful in the analysis of the experimental NMR parameters.

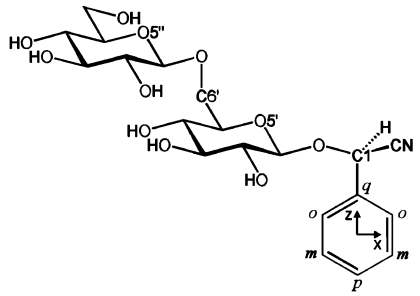

Figure 1. Schematic of amygdalin showing the atom labeling.

2. Materials and Methods

2.1. Materials. Unlabeled amygdalin was obtained from Sigma and used without further purification.

2.2. NMR Experiments. The solid-state experiments were performed at a field of 9.4 T on a Chemagnetics Infinity 400 MHz spectrometer using a 6 mm double-resonance MAS probe. The ^{13}C chemical shifts were externally referenced to TMS by setting the ^{13}C signals of solid adamantane to 29.5 and 38.6 ppm.[12] Typical radio frequency (rf) field strengths were 80 kHz for heteronuclear TPPM decoupling[13] and 45 kHz for ^{13}C. The recycle delay and $^{1}H-^{13}C$ cross-polarization (CP) contact time were 25 s and 1 ms, respectively. The mass of the solid-state NMR samples was ∼200 mg. Additional experimental details are given in section 3.

The principal elements of the ^{13}C chemical shift tensors were determined from spinning-sideband intensities using the two-dimensional (2D) PASS technique,[14] which operates under slow MAS conditions. In this method, the overlapping spinning-sideband manifolds are separated by order. Further details of the 2D PASS sequence can be found elsewhere.[14,15]

Heteronuclear $^{1}H-^{13}C$ dipolar couplings were measured by employing the pulse sequence shown in Figure 2. This 2D experiment was recently introduced by Zhao et al.[16] and achieves high spectral resolution in powders because it operates under

* Corresponding author. Fax: +46-8-152187. E-mail: dick.sandstrom@physc.su.se.
[†] Department of Organic Chemistry.
[‡] Division of Inorganic Chemistry.
[§] Division of Physical Chemistry.

10.1021/jp034306e CCC: $25.00
Published on Web 10/01/2003

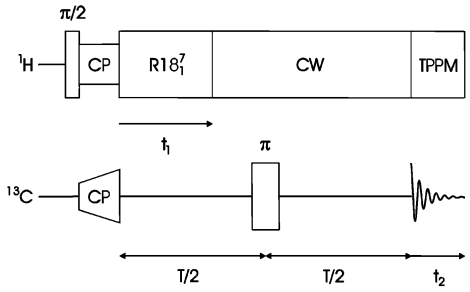

Figure 2. Pulse sequence for 2D separated local field spectroscopy. The experiment correlates scaled ^{1}H−^{13}C dipolar couplings during t_1 with ^{13}C chemical shifts during t_2. Heteronuclear dipolar recoupling is achieved by R18$_1^7$ rf irradiation.

rapid MAS. During the variable evolution period t_1, the CP-enhanced ^{13}C magnetization evolves in the presence of R18$_1^7$ rf irradiation of the protons. This sequence is based on symmetry arguments in MAS NMR[17] and leads to γ-encoded recoupling of ^{1}H−^{13}C dipolar couplings whereas homonuclear dipolar interactions among the ^{1}H spins are suppressed. Proton heteronuclear decoupling is subsequently applied for an interval $T - t_1$ with a ^{13}C π pulse inserted at $T/2$. The duration T is kept constant and equal to an even number of rotor periods. The signal is finally observed during the detection period t_2 as it evolves under the ^{13}C chemical shift interaction and TPPM ^{1}H decoupling. Other NMR methods for measuring ^{1}H−^{13}C dipolar couplings under rapid MAS are also available.[18−22]

Solution NMR spectra of amygdalin dissolved in D_2O or DMSO-d_6 were recorded at 30 °C on Varian Mercury 300 MHz (7.0 T) or 400 MHz (9.4 T) spectrometers, respectively. Carbon-13 resonances were referenced to external dioxane in D_2O at 67.4 ppm.

2.3. Quantum Chemical Calculations. All calculations were carried out on a single amygdalin molecule using the Gaussian 98 (revision A.9) package.[23] The computation of the ^{13}C CS tensors comprised two steps. First, the molecular geometry was optimized at the B3LYP/6-31G(d,p) level of theory. Chemical shift tensor calculations were then performed on the optimized structure, using the gauge-including atomic orbital (GIAO) method[24,25] at the same level of theory.

2.4. Thermal Gravimetric Analysis (TGA). Thermal gravimetry experiments were performed using a Perkin-Elmer TGA7 instrument. The measurements were carried out under air atmosphere at a heating rate of 5 °C/min.

3. Results and Discussion

3.1. ^{13}C Chemical Shift Interactions. Figure 3 shows the conventional ^{13}C CP-MAS spectra (spinning frequency $\omega_r/2\pi$ = 8.0 kHz) of solid amygdalin as a function of temperature. Most of the ^{13}C signals are resolved (at least partially), and several of them may tentatively be assigned by comparison with the solution spectrum. For example, the ^{13}C isotropic chemical shifts (δ_{iso}) of the C1′, C1″, and C6″ sites are close to the liquid-state values. The four aromatic signals obtained at 90 °C may also be assigned on the basis of the solution NMR spectrum. The signal from the cyano group is broad and asymmetrically split by the one-bond ^{14}N−^{13}C dipolar interaction[26] and is therefore easily identified. The spectral region containing the C1, C2′-C6′, and C2″-C5″ peaks (with δ_{iso} values between 66 and 78 ppm) is crowded, and the assignment of these signals is not straightforward. However, for the purpose of studying local mobility in amygdalin, complete assignment of the ^{13}C resonances is not necessary (see below).

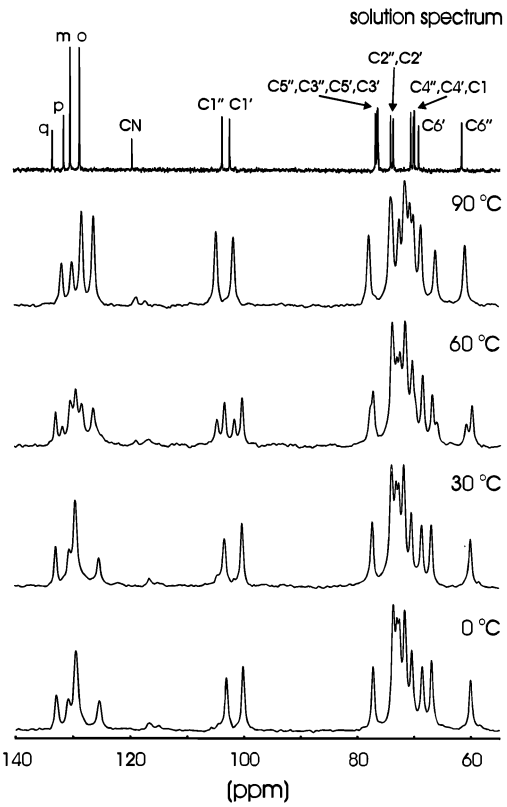

Figure 3. Carbon-13 CP-MAS spectra of amygdalin versus temperature (acquired upon heating). The solution spectrum was recorded under stationary conditions.

An interesting observation in Figure 3 is that the ^{13}C CP-MAS spectra exhibit a distinct temperature dependence. This is most obvious for the spectrum obtained at 60 °C. At this temperature, the C1′, C1″, and C6″ peaks are split with an intensity distribution of about 2:1. This indicates that a molecular repacking takes place, and that these carbons occupy two crystallographically nonequivalent sites. Similar splittings are observed for the aromatic signals.

To determine if the change in the crystal structure is accompanied by changes in molecular mobility, we started by determining ^{13}C chemical shift tensor components at both low (0 °C) and high (90 °C) temperatures. It is well-known that this tensor is a sensitive probe for the study of the local dynamics in solids.[27] The principal elements of the symmetric part of the CS tensors were extracted by a Herzfeld−Berger analysis[28] of the spinning-sideband intensities using the HBA software package.[29] In this work, a deshielding convention for chemical shifts is used. We denote the principal values of the CS tensor by δ_{11} (corresponding to the least shielded direction) ≥ δ_{22} (corresponding to the intermediate shielded direction) ≥ δ_{33} (corresponding to the most shielded direction). The isotropic chemical shift is, using this notation, given by $\delta_{iso} = (\delta_{11} + \delta_{22} + \delta_{33})/3$.

The experimental ^{13}C CS tensor components for the aromatic carbons are given in Table 1 (estimated upon heating). As explained above, the assignment of the ortho (o), meta (m), and para (p) signals is based on a comparison with the solution NMR spectrum. The quaternary (q) peak was unambiguously assigned by ^{1}H−^{13}C dipolar dephasing experiments. It is clear that the aromatic tensors undergo changes when the sample is heated from 0 to 90 °C. The overall width of the CS tensors of the meta and ortho carbons decreases by 20−25%, which indicates the onset of fast ring motions upon heating. Another important

TABLE 1: Experimental ^{13}C Chemical Shift Tensors (ppm) for the Aromatic Carbons in Amygdalin

carbon site	temp (°C)	$\delta_{11} - \delta_{iso}$	$\delta_{22} - \delta_{iso}$	$\delta_{33} - \delta_{iso}$
q	0	95	21	−116
	90	95	5	−100
o	0	90	21	−111
	90	61	37	−98
m	0	99	20	−119
	90	62	41	−103
p	0	100	22	−122
	90	101	8	−109

piece of information is that the δ_{22} and δ_{33} components of the quaternary and para sites are partially averaged by the ring dynamics, whereas the δ_{11} components remain unaffected. This suggests that the phenyl ring motion (i) takes place about the C_2 axis (assuming that this axis coincides with the δ_{11} directions of the quaternary and para carbons) and (ii) differs from a simple 180° flip. The last conclusion is based on the fact that the ^{13}C chemical shift tensors of the quaternary and para carbons are invariant under a 180° reorientation about the C_2 axis.[27] Similar motional processes of phenyl groups have been amply documented in the literature. For example, aromatic ring flipping has been observed in polymers,[6] amino acids,[22] proteins,[30] and molecular crystals.[31]

To obtain an appreciation of the geometry of the local ring motion, we have analyzed the CS tensors in terms of a jump model. This kind of analysis requires knowledge of not only the *magnitudes* but also the *orientations* of the tensor elements. A convenient approach to estimate the orientation of a chemical shift tensor is by using quantum chemical calculations. The results of such calculations for the aromatic carbons in amygdalin are summarized in Table 2. The standard deviation between calculated and experimental ^{13}C CS tensor components obtained at 0 °C is less than 5 ppm (cf. Table 1). Given the experimental error (which we estimate to ±3 ppm at 0 °C) and the fact that the quantum chemical calculations were carried out on an isolated molecule using a moderately sized basis set, this agreement must be considered to be reasonably good. Table 2 also shows that the calculated orientations of the least shielded components (δ_{11}) bisect the C−C−C angle of the phenyl carbons, and that the orientations of the most shielded components (δ_{33}) are perpendicular to the ring plane. This is in agreement with results from previous NMR studies of aromatic ^{13}C chemical shift tensors.[32]

Having estimated the magnitudes (from the solid-state NMR experiments) and orientations (from the quantum chemical calculations) of the aromatic CS tensors, we now analyze them in terms of ring mobility. The procedure for characterizing molecular motions in the solid state by utilizing anisotropic spin interactions such as the ^{13}C chemical shift has been described elsewhere[5,6,33] and will not be repeated here. We assume that the tensor components obtained at low temperatures are motionally unaveraged and that the phenyl ring undergoes a two-site jump about the C_2 axis at high temperatures. Numerical fittings of the CS tensors obtained at 90 °C were performed using the NMR−WebLab program package,[33] and resulted in a jump angle of 145 ± 15°. It should be noted that this dynamical model is by no means unique, but the analysis shows unequivocally that the aromatic ring in amygdalin exhibits large-amplitude motions at elevated temperatures.

To study the local dynamics of the rest of the molecule by measuring ^{13}C chemical shift tensors is more problematic. First,

TABLE 2: Calculated ^{13}C Chemical Shift Tensors for the Aromatic Carbons in Amygdalin[a]

			angles with the ring fixed axes[b]		
carbon site	$\delta_{ii} - \delta_{iso}$	principal values	x	y	z
q	11	87	90	91	1
	22	27	178	92	90
	33	−114	92	2	89
c[c]	11	91	28	89	118
	22	15	62	89	28
	33	−106	92	2	90
o	11	95	151	90	119
	22	17	61	89	151
	33	−112	90	1	89
m	11	98	152	90	62
	22	15	62	90	28
	33	−113	90	180	90
m[c]	11	97	150	90	120
	22	24	120	90	30
	33	−121	90	179	89
p	11	98	89	90	1
	22	17	178	89	89
	33	−115	91	179	90

[a] CS tensor components and angles are in ppm and degrees, respectively. [b] Ring fixed axes are defined in Figure 1. [c] The quantum chemical calculations predict that the two ortho (and the two meta) carbons are nonequivalent.

the magnitudes of ^{13}C CS tensors for sp^3-hybridized carbons are substantially smaller than for sp^2-hybridized aromatic carbons,[32] and the former are therefore slightly more involved to obtain experimentally. Second, and more importantly, to follow and resolve individual ^{13}C signals versus temperature turned out to be difficult in the crowded spectral region between 66 and 78 ppm. To find out whether the glucopyranose rings and linkage groups exhibit local mobility, we decided to measure $^1H-^{13}C$ through-space dipolar couplings in amygdalin. The outcome of such local field experiments is presented below.

3.2. $^1H-^{13}C$ Dipolar Couplings. Cross-sections extracted from two 2D separated local field (SLF) spectra of amygdalin are shown in Figure 4. These slices are dominated by the $^1H-^{13}C$ through-space dipolar interaction between a ^{13}C spin and its directly bonded proton(s). The effect of weaker couplings to more distant protons is minor.[16,34] The only nonprotonated carbons in amygdalin are q and CN, and as expected, cross-sections through the ^{13}C signals from these sites lack a resolved dipolar splitting.

The ortho, meta, and para subspectra obtained at 0 °C exhibit a three-peak structure, where the splitting between the outer two peaks is 6.6 ± 0.2 kHz. Numerical simulations show that this value corresponds to a $^1H-^{13}C$ dipolar coupling of −23.0 ± 0.7 kHz.[35] This matches results from rigid sp^2-hybridized ^{13}C sites[16,22,35] and demonstrates the absence of rapid phenyl ring motions at 0 °C. At the same temperature, the heteronuclear splitting for C1, C1′−C6′, and C1″−C6″ is equal to 6.2 ± 0.2 kHz and corresponds to a dipolar coupling of −21.6 ± 0.7 kHz. This is in agreement with experimental studies of sp^3-hybridized carbons in rigid systems[16,35] and shows that the glucopyranose units and linkage groups are immobile at 0 °C. The difference between the dipolar couplings for the sp^2- and sp^3-hybridized carbons is most likely due to a difference in the carbon−proton bond length for these sites. Using the relationship between the

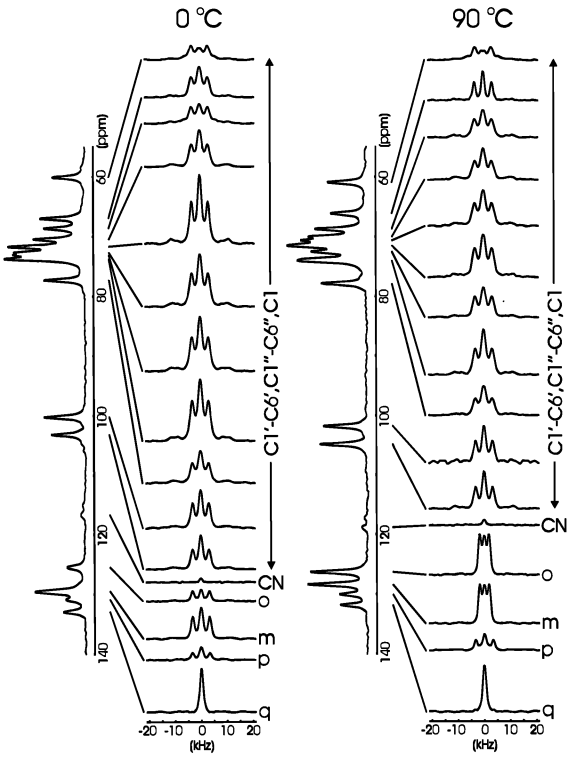

Figure 4. Dipolar cross-sections through two 2D SLF spectra of amygdalin obtained at 0 and 90 °C (recorded upon heating). The spectra were acquired at a spinning frequency of 8.0 kHz using the pulse sequence in Figure 2. The 1D ^{13}C CP-MAS spectra are also shown ($\omega_r/2\pi = 8.0$ kHz).

^{1}H−^{13}C dipolar coupling constant b_{CH} (in Hz) and the C−H distance r_{CH}

$$b_{CH} = -\frac{\mu_0}{8\pi^2}\frac{\gamma_C\gamma_H\hbar}{r_{CH}^3} \quad (1)$$

we find that the effective C−H bond length for an sp^3-hybridized ^{13}C site is approximately 2 pm longer than for an sp^2-hybridized ^{13}C site. This agrees with results from previous solid-state NMR studies[16] and crystal structure data.[36]

If we now turn to the 2D dipolar-shift spectrum obtained at 90 °C (see Figure 4, right column), it is clear that the dipolar splittings for carbons in the glucopyranosyl residues (with δ_{iso} values between 60 and 105 ppm) are unaffected by the sample heating. The heteronuclear splittings for the aromatic ^{13}C sites are, however, significantly different from the ones observed at low temperature. At 90 °C, the ortho and meta subspectra exhibit a dipolar splitting of 3.4 ± 0.2 kHz, whereas the splitting for the para site is 6.6 ± 0.2 kHz. Numerical simulations, assuming a two-site jump model with a jump angle of 160 ± 20°, yielded calculated spectra in agreement with the high-temperature ortho and meta dipolar cross-sections (not shown). These findings clearly show the existence of thermally activated dynamics of the phenyl ring about the C_2 (or para) axis, whereas the rest of the molecule remains static.

Representative results from four 2D SLF experiments carried out between 0 and 90 °C are displayed in Figure 5. The meta and ortho dipolar slices reveal that extensive motions of the aromatic ring take place already at 60 °C.

3.3. Desolvation Upon Heating. Thermal gravimetry experiments showed a mass loss of ca. 10% between 20 and 115 °C. This finding was further substantiated by analysis of the water content in solid amygdalin prior to and after heating at 125 °C for 16 h. The ^{1}H NMR spectra of amygdalin in DMSO-d_6 revealed, by integration of the residual H_2O resonance, that almost 4 water molecules per amygdalin had been lost upon heating. This result correlates well with the TGA measurements.

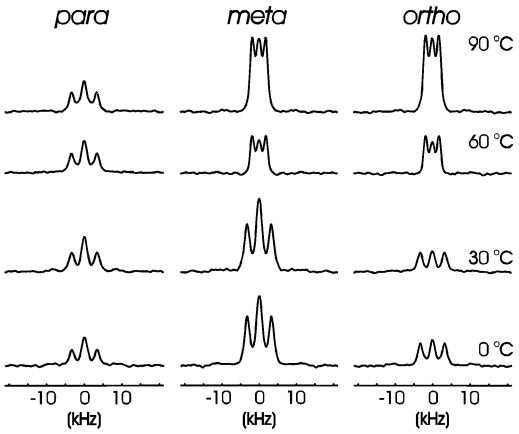

Figure 5. Aromatic dipolar subspectra of amygdalin versus temperature (acquired upon heating). The spectra were recorded at a spinning frequency of 8.0 kHz using the pulse sequence in Figure 2.

All solid-state NMR experiments discussed so far were performed on thermally untreated samples. From the analyses presented above, we know that heating of such samples is accompanied by loss of water, molecular repacking, and onset of phenyl ring dynamics. To study the molecular characteristics upon cooling, we acquired variable-temperature NMR spectra of samples that had been heated at 90 °C for 1 h (not shown). The 1D ^{13}C CP-MAS spectra obtained between 90 and 20 °C were similar to the high-temperature line shape in Figure 3. Furthermore, the meta and ortho dipolar subspectra of thermally treated samples recorded at 30 °C exhibited considerable dynamical averaging. These findings clearly show that the presence (or absence) of water play an important role for the segmental mobility in solid amygdalin.

4. Summary and Conclusions

Carbon-13 MAS NMR spectroscopy provides a means to obtain very detailed information on segmental mobility in disordered solids. In this work, we have presented variable-temperature measurements of ^{13}C chemical shift tensor components and ^{1}H−^{13}C dipolar interactions in the cyanogenic glycoside amygdalin. These anisotropic NMR parameters contain information which is comparable to that of ^{2}H quadrupolar couplings but have the advantage that they can be obtained in unlabeled samples.

The experimental data set obtained upon heating clearly reveals that the phenyl ring in amygdalin exhibits thermally activated dynamics about the C_2 axis. The glucopyranosyl residues are, in contrast, static between 0 and 90 °C. It was also found that heating is accompanied by loss of water from the sample.

In our previous studies of carbohydrates in the solid state we have employed both NMR spectroscopy[37] and X-ray crystallography[38] techniques. To obtain information on molecular structure and dynamics, we will continue to utilize these complementary methods and, in the case of solid-state NMR, develop novel experiments and analytical procedures for a continued and focused investigation of carbohydrate systems being part of or models for those in biological systems such as glycolipids or glycoproteins. A related and important area in which it should be possible to apply solid-state NMR in a fruitful way is the study of carbohydrate-protein interactions.

Acknowledgment. We thank Zheng Weng and Mattias Edén for instrumental and computational help, and Xin Zhao for helpful discussions on R-type pulse sequences. This work was supported by the Swedish Research Council (VR), the Carl Trygger Foundation (CTS), and the Magn. Bergvall Foundation (MBS).

References and Notes

(1) Jones, D. A. *Phytochemistry* **1998**, *47*, 155.
(2) Poulton, J. E. In *Handbook of Natural Toxins: Volume 1*; Keeler, R. F., Tu, A. T., Eds.; Marcel Dekker: Basel, 1983; p 117.
(3) Moertel, C. G.; Fleming, T. R.; Rubin, J.; Kvols, L. K.; Sarna, G.; Koch, R.; Currie, V. E.; Young, C. W.; Jones, S. E.; Davignon, J. P. *N. Engl. J. Med.* **1982**, *306*, 201.
(4) Ribeiro, A. A. *Magn. Reson. Chem.* **1990**, *28*, 765.
(5) Spiess, H. W. *Adv. Polym. Sci.* **1985**, *66*, 23.
(6) Schmidt-Rohr, K.; Spiess, H. W. *Multidimensional Solid-State NMR and Polymers*; Academic Press: London, 1994.
(7) Sandström, D.; Nygren, M.; Zimmermann, H.; Maliniak, A. *J. Phys. Chem.* **1995**, *99*, 6661.
(8) Sandström, D.; Hong, M.; Schmidt-Rohr, K. *Chem. Phys. Lett.* **1999**, *300*, 213.
(9) Torchia, D. A.; Szabo, A. *J. Magn. Reson.* **1982**, *49*, 107.
(10) Wang, Y. L.; Tang, H. R.; Belton, P. S. *J. Phys. Chem. B* **2002**, *106*, 12834.
(11) Nozirov, F.; Szczesniak, E.; Fojud, Z.; Dobrzynski, P.; Klinowski, J.; Jurga, S. *Solid State NMR* **2002**, *22*, 19.
(12) Earl, W. L.; VanderHart, D. L. *J. Magn. Reson.* **1982**, *48*, 35.
(13) Bennett, A. E.; Rienstra, C. M.; Auger, M.; Lakshmi, K. V.; Griffin, R. G. *J. Chem. Phys.* **1995**, *103*, 6951.
(14) Antzutkin, O. N.; Shekar, S. C.; Levitt, M. H. *J. Magn. Reson. A* **1995**, *115*, 7.
(15) *Solid-State NMR Spectroscopy: Principles and Applications*; Duer, M. J., Ed.; Blackwell Science: Oxford, U.K., 2002.
(16) Zhao, X.; Edén, M.; Levitt, M. H. *Chem. Phys. Lett.* **2001**, *342*, 353.
(17) Levitt, M. H. In *Encyclopedia of Nuclear Magnetic Resonance: Supplementary Volume*; Grant, D. M.; Harris, R. K., Eds.; John Wiley & Sons: Chichester, U.K., 2002; p 165.
(18) McElheny, D.; DeVita, E.; Frydman, L. *J. Magn. Reson.* **2000**, *143*, 321.
(19) van Rossum, B. J.; de Groot, C. P.; Ladizhansky, V.; Vega, S.; de Groot, H. J. M. *J. Am. Chem. Soc.* **2000**, *122*, 3465.
(20) Saalwächter, K.; Spiess, H. W. *J. Chem. Phys.* **2001**, *114*, 5707.
(21) Wind, M.; Wiesler, U. M.; Saalwächter, K.; Müllen, K.; Spiess, H. W. *Adv. Mater.* **2001**, *13*, 752.
(22) Hong, M.; Yao, X.; Jakes, K.; Huster, D. *J. Phys. Chem. B* **2002**, *106*, 7355.
(23) Frisch, M. J.; Trucks, G. W.; Schlegel, H. B.; Scuseria, G. E.; Robb, M. A.; Cheeseman, J. R.; Zakrzewski, V. G.; Montgomery, J. A.; Stratmann, R. E.; Burant, J. C.; Dapprich, S.; Millam, J. M.; Daniels, A. D.; Kudin, K. N.; Strain, M. C.; Farkas, O.; Tomasi, J.; Barone, V.; Cossi, M.; Cammi, R.; Mennucci, B.; Pomelli, C.; Adamo, C.; Clifford, S.; Ochterski, J.; Petersson, G. A.; Ayala, P. Y.; Cui, Q.; Morokuma, K.; Malick, D. K.; Rabuck, A. D.; Raghavachari, K.; Foresman, J. B.; Cioslowski, J.; Ortiz, J. V.; Stefanov, B. B.; Liu, G.; Liashenko, A.; Piskorz, P.; Komaromi, I.; Gomperts, R.; Martin, R. L.; Fox, D. J.; Keith, T.; Al-Laham, M. A.; Peng, C. Y.; Nanayakkara, A.; Gonzales, C.; Challacombe, M.; Gill, P. M. W.; Johnson, B. G.; Chen, W.; Wong, M. W.; Andres, J. L.; Head-Gordon, M.; Replogle, E. S.; Pople, J. A. *Gaussian 98*, Revision A.9; Gaussian Inc.: Pittsburgh, PA, 1998.
(24) Ditchfield, R. *Mol. Phys.* **1974**, *27*, 789.
(25) Wolinski, K.; Hinton, J. F.; Pulay, P. *J. Am. Chem. Soc.* **1990**, *112*, 8251.
(26) Hexem, J. G.; Frey, M. H.; Opella, S. J. *J. Chem. Phys.* **1982**, *77*, 3847.
(27) Schaefer, J.; Stejskal, E. O.; McKay, R. A.; Dixon, W. T. *Macromolecules* **1984**, *17*, 1479.
(28) Herzfeld, J.; Berger, A. E. *J. Chem. Phys.* **1980**, *73*, 6021.
(29) Eichele, K.; Wasylishen, R. E. *HBA: Herzfeld-Berger Analysis Program*, version 1.4; Dalhousie University: Halifax, Canada, 2001.
(30) Wüthrich, K. *NMR of Proteins and Nucleic Acids*; John Wiley & Sons: New York, 1986.
(31) Stumber, M.; Zimmermann, H.; Schmitt, H.; Haeberlen, U. *Mol. Phys.* **2001**, *99*, 1091.
(32) Veeman, W. S. *Prog. NMR Spectrosc.* **1984**, *16*, 193.
(33) Macho, V.; Brombacher, L.; Spiess, H. W. *Appl. Magn. Reson.* **2001**, *20*, 405.
(34) Zhao, X.; Sudmeier, J. L.; Bachovchin, W. W.; Levitt, M. H. *J. Am. Chem. Soc.* **2001**, *123*, 11097.
(35) Dvinskikh, S. V.; Luz, Z.; Zimmermann, H.; Maliniak, A.; Sandström, D. *J. Phys. Chem. B* **2003**, *107*, 1969.
(36) *International Tables for Crystallography: Volume C*; Wilson, A. J. C., Ed.; Kluwer: Dordrecht, The Netherlands, 1995; p 696.
(37) Ravindranathan, S.; Karlsson, T.; Lycknert, K.; Widmalm, G.; Levitt, M. H. *J. Magn. Reson.* **2001**, *151*, 136.
(38) Färnbäck, M.; Eriksson, L.; Widmalm, G. *Acta Crystallogr.* **2003**, *C59*, 171.